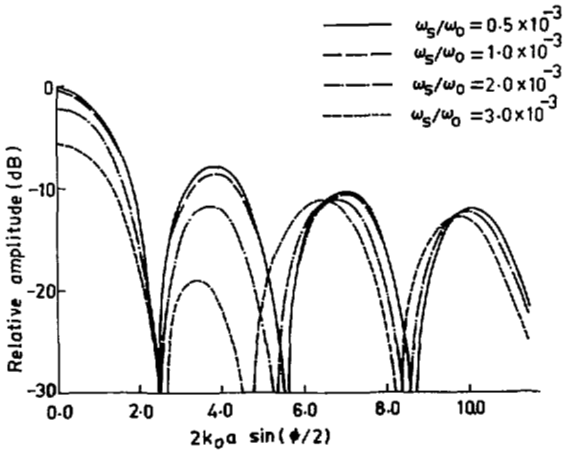

Fig. 3. Circular array radiation pattern for different values of ω_s/ω_0.

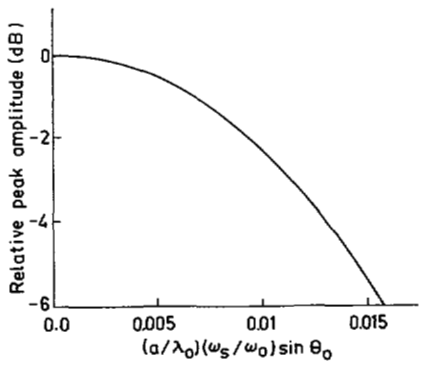

Fig. 4. Loss of peak amplitude with scanning rate.

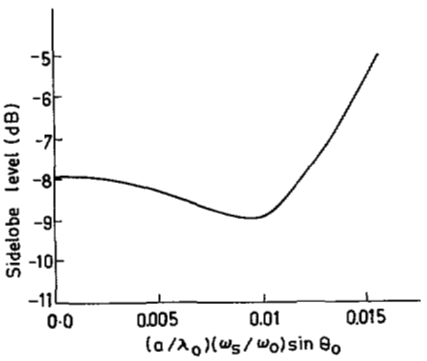

Fig. 5. Variation of sidelobe level with scanning rate.

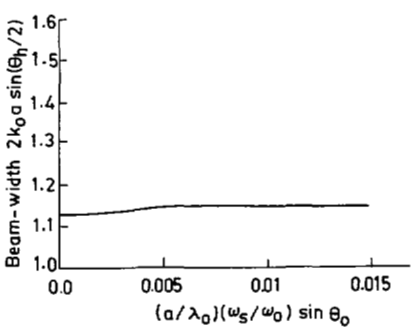

Fig. 6. Array beamwidth versus scanning rate.

of the circular array. However, unlike the linear array, the circular array does not exhibit any significant change in the 3 dB bandwidth, nor does it show a frequency spread associated with a fast scanning linear array. Examples from both radar and sonar have been considered.

REFERENCES

[1] R. E. Collin and F. J. Zucker, *Antenna Theory, Part 1*. New York: McGraw-Hill, 1969.
[2] E. A. Wolff, *Antenna Analysis*. New York: Wiley, 1966.
[3] R. W. P. King, R. B. Mack, and S. S. Sandler, *Arrays of Cylindrical Dipoles*. London: Cambridge Univ. Press, 1968.
[4] P. W. James, "Polar patterns of phase-corrected circular arrays," *Proc. Inst. Elec. Eng.*, vol. 112, no. 10, pp. 1839–1848, Oct. 1965.
[5] D. E. N. Davies and B. S. McCartney, "Cylindrical arrays with electronic beam scanning," *Proc. Inst. Elec. Eng.*, vol. 112, no. 3, pp. 497–505, Mar. 1965.
[6] R. G. Fenby and D. E. N. Davies, "Circular array providing fast 360° electronic beam rotation," *Proc. Inst. Elec. Eng.*, vol. 115, no. 1, pp. 78–86, Jan. 1968.
[7] V. D. Agrawal and R. K. Arora, "Scanning transients in phased array antennas," *Proc. IEEE*, vol. 62, no. 6, pp. 850–851, June 1974.
[8] R. K. Arora and V. D. Agrawal, "Frequency-spread associated with fast electronic scanning," *Proc. IEEE*, vol. 62, no. 8, pp. 1175–1176, Aug. 1974.
[9] G. N. Watson, *A Treatise on the Theory of Bessel Functions*, 2nd ed. London: Cambridge Univ. Press, 1966.
[10] M. R. Patel and R. K. Arora, "Radiation distortions in fast frequency-scanned antenna arrays," *IEEE Trans. Antennas Propagat.*, vol. AP-24, no. 4, pp. 537–539, July 1976.

Tracking Antenna Arrays for Near-Millimeter Waves

PETER P. TONG, DEAN P. NEIKIRK, DEMETRI PSALTIS, MEMBER, IEEE, DAVID B. RUTLEDGE, MEMBER, IEEE, KELVIN WAGNER, AND PETER E. YOUNG

Abstract—**A two-dimensional monolithic array has been developed that gives the elevation and azimuth of point source targets. The array is an arrangement of rows and columns of antennas and bismuth bolometer detectors on a fused quartz substrate. Energy is focused onto the array through a lens placed on the back side of the substrate. At 1.38 mm with a 50 mm diameter objective lens, the array has demonstrated a positioning accuracy of 26 arcmin. In a differential mode this precision improves to 9 arcsec, limited by the mechanics of the rotating stage. This tracking could be automated to a fast two-step procedure where a source is first located to the nearest row and column, and then precisely located by scanning. With signal processing the array should be able to track multiple sources.**

FAR-INFRARED AND MILLIMETER-WAVE IMAGING

Recently, imaging antenna arrays have been developed that make one-dimensional line images at far-infrared and millimeter wavelengths [1]–[3]. The idea is that an image is focused on a line array of antennas with individual detectors. The power received by each antenna is plotted to form a one-dimensional

Manuscript received August 2, 1982; revised December 7, 1982. This work was supported by the Jet Propulsion Laboratory under Account 49-730-00209-0-3830 and by the Department of Energy under Contract DE-AM03-76SF-00010, Task IIA.

P. P. Tong, D. P. Neikirk, D. Psaltis, D. B. Rutledge, and K. Wagner are with the Division of Engineering and Applied Science, California Institute of Technology, Pasadena, CA 91125.

P. E. Young is with the Department of Electrical Sciences and Engineering, University of California, Los Angeles, CA 90024.

0018-926X/83/0500-0512$01.00

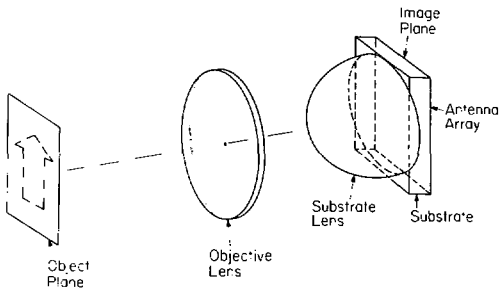

Fig. 1. Substrate-lens coupled optical system.

image. Fig. 1 shows how these systems are put together. An objective lens focuses the image onto the array through a lens placed on the back of the substrate. This substrate lens takes advantage of the fact that antennas on a substrate are most sensitive to radiation from the substrate side. These one-dimensional arrays are useful for many purposes, but other applications will require two-dimensional information. The one-dimensional array could be extended to make a two-dimensional array, but in the present form, separate low-frequency connections are required for each detector so that many leads would be needed. In the future it may be possible to develop this wiring, or to build circuitry similar to charge-coupled devices to make it unnecessary. For the present, we have developed a two-dimensional array that requires low-frequency leads only for each row and column of antennas. A price is paid, however, in that the array does not give complete images, but it does give two-dimensional tracking information (the elevation and azimuth) for point sources.

TRACKING ARRAYS

Figs. 2 and 3 show a tracking array designed for a wavelength of 1.2 mm. The array consists of rows and columns of 60° bow-tie antennas [1]-[3] and bolometer detectors [4] connected in series. Because of the series connection, the signal measured on the low-frequency leads gives the total power received along a particular row or column. The strongest column signal gives the source azimuth, and the strongest row signal gives the source elevation. More precise tracking information can be obtained by taking the difference between adjacent row and column signals in a way similar to optical centroid trackers [5] and microwave monopulse receivers [6]. In order to get this improvement, however, the array must be wobbled slightly to null the difference signal.

This array can locate a single point source, and the question that naturally arises is, what happens when there are more point sources? If the sources all have different intensities, azimuths, and elevations, the array could track them simultaneously by identifying the row and column signals with equal magnitudes. If intensities, azimuths, or elevations are equal, there will be ambiguities. In a dynamic situation, these ambiguities may only persist for short periods of time, and with appropriate processing, multiple-target tracking should be feasible. It should also be possible to follow a single source when other sources pass through in the field of view of the array.

There is an interesting connection between the tracking array and X-ray transaxial tomographic imaging. The information produced by the array is the projections of the image along two perpendicular axes. The ambiguities that arise from sources of equal intensities, azimuths, and elevations, could be resolved in principle by rotating the array about the optical axis to produce different projections. In some applications, such as missile guidance, the platform may rotate anyway. In principle, an arbitrary image can be reconstructed from its projections, similar to the way it is done in X-ray transaxial tomographic imaging [7].

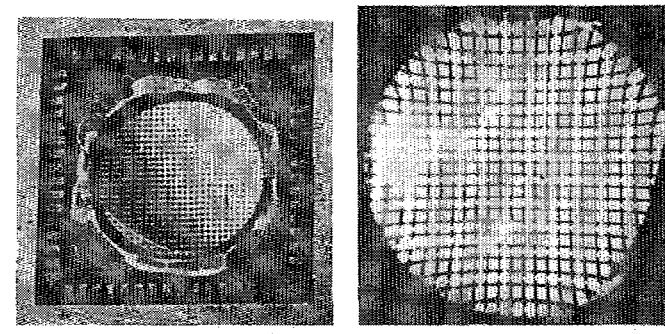

(a) (b)

Fig. 2. Tracking array. (a) View from the air side showing standard DIP package. (b) View through substrate lens.

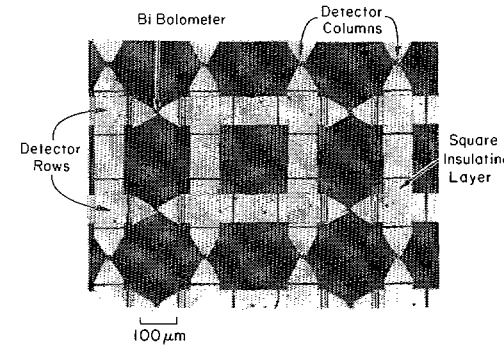

Fig. 3. Micrograph of a tracking array designed for 1.2 mm. The antennas are made of silver, and appear light. The fused-quartz substrate appears dark. The distance between adjacent rows (or columns) is 268 μm ($7/16\lambda_d$) and the distance between adjacent detectors in a single row or column is 535 μm ($7/8\lambda_d$). At its widest, the silver is 80 μm wide ($2/15\lambda_d$). Overlapping rows and columns are insulated from each other by a layer of polyimide.

The number of antennas and detectors in a row or column affects the array sensitivity. This arrangement, where the output of a group antennas and detectors is combined, is called a multimode antenna [8]. A general property of multimode antennas is that the sensitivity degrades as the number of detectors increases. For the series-connected rows and columns, this is easy to understand because the total noise of a row or column is larger than the noise of a single detector. In terms of the noise equivalent power (NEP), the NEP of a row or column of n detectors is $\sqrt{n}$ times the NEP of a single device.

MICROWAVE DESIGN

The array was designed by building large-scale microwave models. The model antennas were made of copper foil and the substrate was artificial dielectric with a dielectric constant of four to match the fused quartz substrates used at near-millimeter wavelengths. The antennas were isolated from each other at low frequencies by masking tape. The spacing between rows and columns must be small enough so that the resolution does not degrade. Previous work [1]-[4] show that $\lambda_d/2$ spacing is adequate. The dimensions were chosen by trial and error to give adequate impedance and radiation patterns.

The impedance of the model is important because impedance cannot be conveniently measured at 1.2 mm. It indicates the coupling efficiency for different kinds of detectors and the avail-

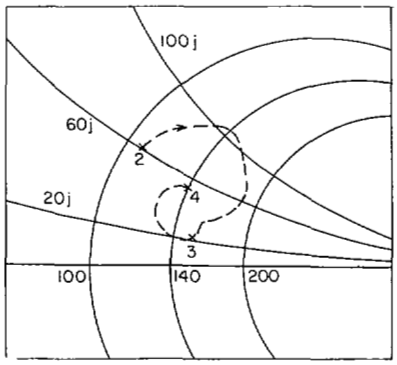

Fig. 4. Detector embedding impedance of a large-scale model, plotted from 2 to 4 GHz on a Smith chart.

able bandwidth. Fig. 4 shows the model embedding impedance in ohms from 2 to 4 GHz. At the design frequency, 3 GHz, the impedance was $150 + j20\ \Omega$. The resonance is weak, and this should be an adequate impedance for matching to either Schottky diodes or bolometers over a large bandwidth.

The radiation patterns of the array indicate how efficiently energy will be coupled into the array, and also help determine the optical system. These patterns are needed because it is difficult to make accurate coupling efficiency measurements at near-millimeter wavelengths. Fig. 5 shows the radiation patterns into the substrate measured at a single detector in the array. The pattern for radiation into the air is at least 10 dB below the peak substrate power and is omitted. The patterns show a symmetrical beam with a half-power beamwidth of 30° and the E-plane pattern shows large sidelobes that could not be eliminated.

NEAR-MILLIMETER TESTING

The array is made by conventional contact lithography and lift-off [2]. The silver antennas were 800 Å thick. A half-micron polyimide insulating layer, Dupont Pyrallin 2555, was spun on between successive silver evaporations. Then 3000 Å Bi-bolometers were deposited. The particular array used in testing had bolometer resistances in the range 15 to 25 Ω. This is a poor match to the antenna but the resulting signal levels were sufficient to demonstrate the array properties. The bolometer is convenient for testing antennas and arrays but its sensitivity (NEP $\sim 10^{-9}$W/$\sqrt{\text{Hz}}$) is not good enough for many applications. Most of these applications would require that the bolometer be replaced by a Schottky diode. After fabrication the arrays were mounted in a standard dual in-line package (DIP). The full array is 32 × 32, and this size can be adjusted during wire bonding. In our experiment the arrays were 7 × 7. The fused quartz substrate lens had a radius of curvature of 6.62 mm, and the lens-substrate combination had a thickness of 10 mm. The TPX objective lens had a 70 mm focal length and a 50 mm diameter.

Fig. 6 shows the system patterns at 1.22 mm. The H-plane pattern is generated when the focused spot scans across a row. This pattern is sharply peaked, resembling the Airy pattern of the optical system [9]. The E-plane pattern results when the focused spot scans along a row from detector to detector. Ideally this signal should be constant, but Fig. 6 shows some roll-off, probably resulting from lens aberrations and differences in bolometers.

The next measurement demonstrated the tracking ability of the array. The source, a klystron at 1.38 mm, was translated in a plane 70 cm from the array. The power incident on the objective lens was 0.4 mW, and the output signal maxima were about 30 μV. The positions of the maxima were determined by standard sincfunction interpolation [2]. Fig. 7 compares the measured positions in the image plane with the predictions of geometrical optics. The average error in the image plane was 160 μm, and corresponding error in the far field was 26 arcmin. This is five times smaller than the diffraction-limited Rayleigh resolution limit for a pair of point sources.

Much more precise tracking information can be obtained by taking the difference between adjacent row or column signals. As a function of angle, this pattern (Fig. 8) is just the difference between two overlapping H-plane system patterns. It was measured with the differential inputs of a PAR-124 lock-in amplifier. The actual tracking procedure is similar to that of monopulse radars and optical centroid trackers where the system must be oriented

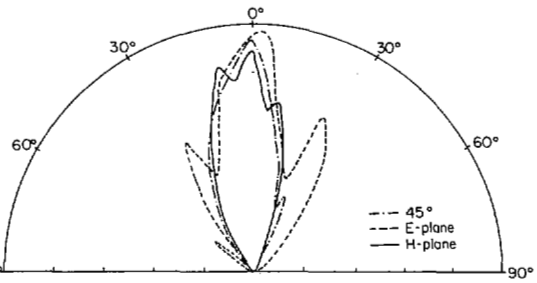

Fig. 5. Feed patterns measured at a single detector diode at 10 GHz on a scale model. The plot is linear in power.

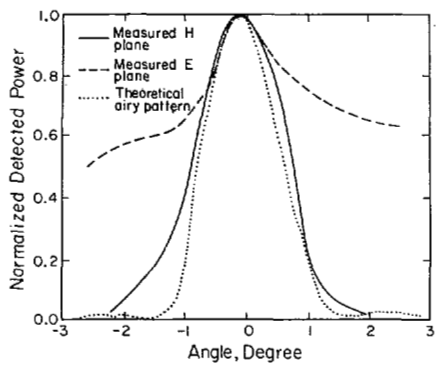

Fig. 6. Near-millimeter system patterns. The source was a CO_2-pumped C_{13} methyl-fluoride laser.

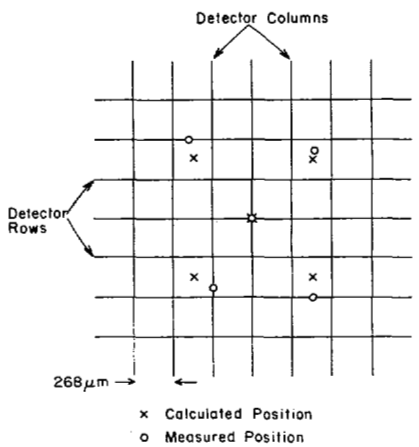

Fig. 7. Tracking demonstration. The grid shows the locations of the detector rows and columns.

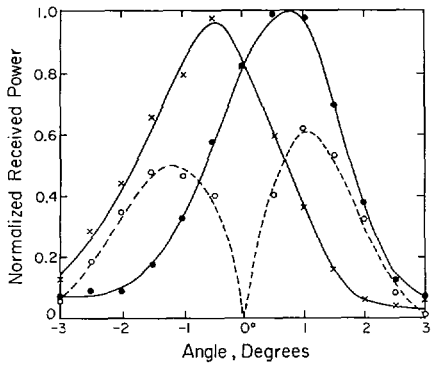

Fig. 8. Magnitude of the difference pattern of adjacent rows (ooo), along with the two overlapping H-plane system patterns (xxx and •••). The difference signal charges sign on each side of the null.

to null the difference pattern. We were able to orient the system toward the source with an accuracy of 9 arcsec, as indicated by the resulting difference signal. This accuracy was limited by the mechanics of the rotating stage rather than the system signal-to-noise ratio.

CONCLUSION

A monolithic two-dimensional tracking array with a 50 mm diameter lens has demonstrated at 1.38 mm a mean positioning error of 160 μm in the image plane, and 26 arcmin in the far field. In the differential mode the array can be oriented to 9arc-sec, limited by the mechanics of the rotating stage. With this array, one can envision a fast two-step tracking procedure. First, the signal maxima would locate the source to a particular row and column. Then the array would scan in the difference mode to track the source precisely. This would be much faster than simply scanning the array to two dimensions. The array, with processing, could track multiple targets.

ACKNOWLEDGMENT

We would like to thank Professor Neville Luhmann of UCLA for the use of equipment and facilities, and Dr. Tom Galantowicz, Mr. Ray Calloway and Mr. Eric Fletcher of the Aerospace Corporation for the loan of the klystron and their help with measurements. Also we appreciate Professor S. E. Schwarz, Mr. Tat Choi, Mr. Davis Hass, and Mr. Simon Tam of the University of California, Berkeley, for their help in making mask.

REFERENCES

[1] D. B. Rutledge and M. S. Muha, "Imaging antenna arrays," *IEEE Trans. Antennas Propagat.*, vol. 30, pp. 535–540, 1982.
[2] D. P. Neikirk, D. B. Rutledge, M. S. Muha, H. Park, and C. X. Yu, "Far infrared imaging antenna arrays," *Appl. Phys. Lett.*, vol. 40, pp. 203–205, 1982.
[3] D. P. Neikirk, P. P. Tong, D. B. Rutledge, H. Park, and P. E. Young, "Imaging antenna array at 119μm," *Appl. Phys. Lett.*, vol. 41, pp. 329–331, 1982.
[4] T. L. Hwang, S. E. Schwarz, and D. B. Rutledge, "Microbolometers for infrared detection," *Appl. Phys. Lett.*, vol. 34, pp. 773–776, 1979.
[5] C. M. Crocker, Jr., "Wide dynamic range instrument for measurement of laser spot position on stationary and moving targets," *Proc. Soc. Photo-Opt. Instrum. Eng.*, vol. 255, pp. 69–72, 1980.
[6] M. I. Skolnik, *Radar Handbook*. New York: McGraw-Hill, 1970, ch. 21.
[7] H. Barrett and W. Swindell, "Analog reconstruction methods for transaxial tomography," *Proc. IEEE*, vol. 65, p. 89, 1977.
[8] D. B. Rutledge and S. E. Schwarz, "Planar multimode detector arrays for infrared and millimeter-wave applications," *IEEE J. Quantum Electron.*, vol. QE-17, pp. 407–414, 1981.
[9] J. W. Goodman, *Introduction to Fourier Optics*. New York: McGraw-Hill. p. 64, 1968.

On the Current Distribution for Open Surfaces

EDWARD H. NEWMAN, MEMBER, IEEE, AND MARK R. SCHROTE

Abstract—**The solution of electric and magnetic field type integral equations is investigated for a simple open surface, i.e., a thin plate. By combining the electric and magnetic field formulations, a set of coupled integral equations is obtained which can be solved for the currents on either side of the plate. Numerical results illustrate these currents for different size plates.**

I. INTRODUCTION

The current distribution on open or closed surfaces can be obtained via the solution of the appropriate electric or magnetic field type integral equation. The solution of these equations is investigated for a thin plate which is a simple example of an open surface. It is shown that the electric field formulations result in the sum current which radiates the correct scattered field. Magnetic field formulations result in a difference current, which do not radiate the scattered field. By combining the electric and magnetic field formulations, a pair of coupled integral equations is obtained which can be solved for the currents on either side of the plate. Numerical results illustrate how these currents, induced by a normally incident plane wave, are affected by plate size.

II. THEORY

In this section we will develop integral equations for the current distribution on an open surface. In particular, the equations will permit the explicit computation of the currents on either side of the open surface.

Fig. 1 shows the side view of a typical open surface, i.e., a flat plate. The plate is shown with a thickness t so that the two sides or surfaces of the plate can be shown, and so that the surface equivalence theorem can be used. However, we will be considering the limiting case as $t \to 0$. Thus, the open surface is considered as a limiting case of a closed surface, i.e., as the thickness t goes to zero. S will denote the closed surface enclosing the plate. Currents on the sides of thickness t will be ignored.

In the ensuing discussion we will use the following notation.

S_T Top surface of S.
S_B Bottom surface of S.
$\mathbf{J}$ Current flowing on the surface S.
$\mathbf{J}_T$ Top current, i.e., that portion of $\mathbf{J}$ on S_T.
$\mathbf{J}_B$ Bottom current, i.e., that portion of $\mathbf{J}$ on S_B.
$\mathbf{J}_S$ Sum current, i.e., a single surface current equal to the

Manuscript received August 30, 1982, revised November 12, 1982. This work was supported in part by the Joint Services Electronics Program and in part by The Ohio State University Research Foundation under Contract N00014-78-C-0049.

The authors are with the ElectroScience Laboratory, Department of Electrical Engineering, The Ohio State University, Columbus, OH 43212.